

# Staggered Spin Order of Localized $\pi$ -electrons in the Insulating State of the Organic Conductor $\kappa$ -(BETS)<sub>2</sub>Mn[N(CN)<sub>2</sub>]<sub>3</sub>

O. M. Vyaselev<sup>1)</sup>, M. V. Kartsovnik\*, N. D. Kushch<sup>+</sup>, E. B. Yagubskii<sup>+</sup>

*Institute of Solid State Physics of the RAS, 142432 Chernogolovka, Russia*

*\*Walther-Meissner-Institut, Bayerische Akademie der Wissenschaften, 85748 Garching, Germany*

*<sup>+</sup>Institute of Problems of Chemical Physics of the RAS, 142432 Chernogolovka, Russia*

Submitted 18 April 2023

Magnetic properties of the conduction  $\pi$ -electron system of  $\kappa$ -(BETS)<sub>2</sub>Mn[N(CN)<sub>2</sub>]<sub>3</sub> have been probed using <sup>13</sup>C NMR. At ambient pressure, the metal-insulator transition observed in the resistivity measurements below  $T \simeq 23$  K is shown to be accompanied by ordering of the  $\pi$ -spins in a long-range staggered structure. As the metal-insulator transition is suppressed by applying a small pressure of  $\sim 0.5$  kbar, the  $\pi$ -spin system maintains the properties of the metallic state down to 5 K.

The organic charge-transfer salt  $\kappa$ -(BETS)<sub>2</sub>Mn[N(CN)<sub>2</sub>]<sub>3</sub> [1] is a quasi-two-dimensional metal consisting of insulating layers of Mn[N(CN)<sub>2</sub>]<sub>3</sub><sup>-</sup> polymer anions alternating with conducting layers of dimers of organic radical cations BETS [bis(ethylenedithio)tetraselenafulvalene, C<sub>10</sub>S<sub>4</sub>Se<sub>4</sub>H<sub>8</sub>] molecules (Fig. 1). The bulk magnetic properties

(MI) transition at cooling below  $T_{\text{MI}} \sim 23$  K at ambient pressure [1]. The transition temperature rapidly decreases at applying pressure,  $P$ , so that at  $P \geq 1$  kbar the system is metallic in the whole temperature range [3]. Moreover, it goes superconducting with maximum  $T_c = 5.8$  K at  $P = (0.6-1.0)$  kbar.

Much effort has been done recently to understand the influence of paramagnetic  $d$ -metal ions of the anion layers on the transport properties of quasi-two-dimensional systems [4, 5]. It has been undoubtedly established now that the field-induced superconductivity in  $\lambda$ -(BETS)<sub>2</sub>FeCl<sub>4</sub> and  $\kappa$ -(BETS)<sub>2</sub>FeBr<sub>4</sub> arises when the external magnetic field compensates the exchange field created by localized  $3d$  moments of Fe<sup>3+</sup> on the spins of itinerant  $\pi$ -electrons [6]. The role of  $\pi$ - $d$  interactions in driving the MI transition observed in the systems with magnetic anions is not as clear. For example, at ambient pressure and zero field, non-magnetic (BETS)<sub>2</sub>Ga(Cl,Br)<sub>4</sub> systems are metallic down to lowest temperatures, whereas the iron-containing  $\kappa$ -(BETS)<sub>2</sub>Fe(Cl,Br)<sub>4</sub> are metallic below the antiferromagnetic (AF) transition, and  $\lambda$ -(BETS)<sub>2</sub>FeCl<sub>4</sub> is a uniaxial Néel-type AF insulator below  $T_N = T_{\text{MI}} = 8$  K [5]. It has been suggested [7] that in the above-mentioned Fe-containing systems the AF state is initiated within the system of  $3d$  electron spin moments of Fe<sup>3+</sup> ions, which in the case of  $\lambda$ -(BETS)<sub>2</sub>FeCl<sub>4</sub> drives the MI transition as well. This reasonable assumption has been doubted however in later communications [8, 9].

Despite the similarity of the title compound to the listed systems with FeX<sub>4</sub> (X=Cl, Br) anions, including the presence of the  $3d$  ions in the anion layer and the MI transition, its phase diagram is different. First, at ambient pressure the system remains insulating in the

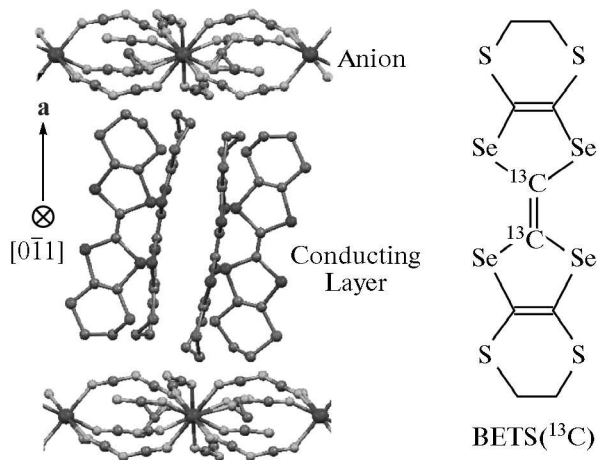


Fig. 1. The crystal structure of  $\kappa$ -(BETS)<sub>2</sub>Mn[N(CN)<sub>2</sub>]<sub>3</sub> viewed along  $[0\bar{1}1]$  direction (left), and the BETS(<sup>13</sup>C) molecule with <sup>13</sup>C isotope in the positions of the central carbon sites (right)

of the system are dominated by the paramagnetic  $3d$  electron spin moments of Mn<sup>2+</sup> ions ( $S_d = 5/2$ ,  $g \approx 2$ ) located in the anion layers [1, 2]. The (BETS)<sub>2</sub><sup>+</sup> dimers accommodating one hole per dimer, form an effectively half-filled quasi-two-dimensional  $\pi$ -electron conduction band [3]. The compound undergoes a metal-insulator

<sup>1)</sup> e-mail: vyasel@issp.ac.ru

external magnetic field up to at least 15 T with no sign of the field-induced superconductivity. Secondly, its bulk dc magnetization does not demonstrate a pronounced AF transition [2]. A feasible reason for the latter is considerably different structure of its anion layer. In the iron-based compounds, it is a rectangular network of discrete paramagnetic units  $\text{FeX}_4^-$ , so that the exchange coupling between  $\text{Fe}^{3+}$  ions is mediated by  $\pi$ -electrons of cation layers [7]. In  $\kappa\text{-(BETS)}_2\text{Mn}[\text{N}(\text{CN})_2]_3$ , the Mn atoms are arranged in isosceles triangles, a geometry that is frustrating for an antiparallel spin order. Besides, the  $\pi$ -electrons are not necessarily involved into the exchange interaction between  $\text{Mn}^{2+}$  ions linked within the polymeric anion layer via dicyanamide bridges [1].

In fact, below the MI transition the bulk static susceptibility of  $\kappa\text{-(BETS)}_2\text{Mn}[\text{N}(\text{CN})_2]_3$  deviates slightly from the Curie–Weiss law obeyed accurately above  $T_{\text{MI}}$ . Gradually decreasing compared to the Curie–Weiss value,  $\chi_{\text{CW}}(T)$ , the susceptibility becomes 80–85% of  $\chi_{\text{CW}}$  at  $T = 2$  K [2]. Combined with the results of  $^1\text{H}$  NMR [10] this infers some disordered tilt of the static component of  $\text{Mn}^{2+}$  moments from the external field direction. This could possibly result from the trend of the  $\text{Mn}^{2+}$  system towards AF order, frustrated geometrically by the triangular arrangement of Mn in the anion layer. This magnetic effect occurs just below the MI transition temperature indicating the existence of the coupling between  $d$  electrons of  $\text{Mn}^{2+}$  and the conduction  $\pi$ -electrons. However, the small size of this effect and its gradual character (compared to the steep resistivity growth below  $T_{\text{MI}}$ ) makes it unlikely to be a driving force for the MI transition. Besides, the magnetic torque measurements have given a hint of a magnetic order within  $\pi$ -electrons below the MI transition [2]. This favors a MI transition scenario more typical for quasi-two-dimensional conductors with half-filled band which involves strong correlations within the  $\pi$ -electrons leading to a Mott instability [11], as it has been suggested in [2, 3].

An insight into the properties of the  $\pi$ -electron spin system is important for illuminating this issue. Invisible in the bulk magnetization measurements due to the masking effect from  $\text{Mn}^{2+}$  moments, the  $\pi$ -spin system can be effectively probed using NMR on the “central” carbons of the BETS molecule, Fig. 1 [12]. In this paper we report the results of  $^{13}\text{C}$  NMR experiments on  $\kappa\text{-(BETS)}_2\text{Mn}[\text{N}(\text{CN})_2]_3$  performed at ambient pressure and under an external pressure sufficient to suppress the MI transition.

The sample was a single crystal of  $\kappa\text{-(BETS)}_2\text{Mn}[\text{N}(\text{CN})_2]_3$  with BETS molecules containing (at least) 99% of  $^{13}\text{C}$  isotope in the positions

of the central carbons, Fig. 1. The sample size was  $a^* \times b \times c \sim 0.05 \times 3 \times 3$  mm<sup>3</sup>.  $\kappa\text{-(BETS)}_2\text{Mn}[\text{N}(\text{CN})_2]_3$  crystals were synthesized by electrochemical oxidation of the  $^{13}\text{C}$ -labeled BETS in the presence of the complex salt  $\text{Ph}_4\text{PMn}[\text{N}(\text{CN})_2]_3$  as electrolyte according to the procedure described in Ref. [13]. The sample was suspended inside a  $5 \times 5 \times 0.5$  mm<sup>3</sup> NMR rf coil on four  $10 \mu\text{m}$ -thick platinum leads attached to the sample to provide the resistivity measurements across the conducting ( $b, c$ ) plane, and sealed inside a PTFE can. To impose the external pressure to the sample, the can was filled with GKZh-136 silicone liquid which is known to generate at low temperatures a pressure of several hundred bar due to the difference in thermal contractions [14]. To testify the pressure generated inside the sample, the resistance of the sample with and without GKZh-136 was measured in the external field  $\mu_0 H = 7$  T in the same cooling cycles with NMR measurements. Figure 2 demonstrates essential sup-

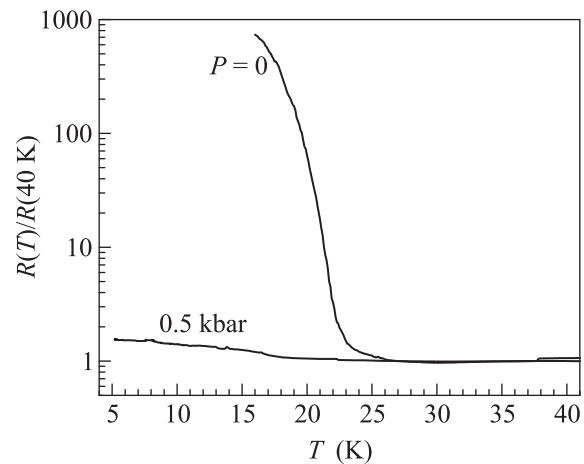


Fig. 2. Temperature dependences of the interplane resistivity of  $\kappa\text{-(BETS)}_2\text{Mn}[\text{N}(\text{CN})_2]_3$  crystal at ambient pressure and under a pressure of  $\sim 0.5$  kbar, measured in the external field  $\mu_0 H = 7$  T

pression of the MI transition in the sample submerged in GKZh-136 implying a pressure of at least 0.5 kbar generated in the sample [3].

NMR was measured in field  $\mu_0 H = 7$  T aligned perpendicular to  $[0\bar{1}1]$  diagonal at angle  $45^\circ$  with  $\mathbf{a}^*$  direction. The spectra were acquired using a standard spin-echo sequence with  $\pi$ -pulse length  $\leq 2.5 \mu\text{s}$ . To cover broad spectra, Fourier-transforms of the acquired spin-echoes were collected at intervals  $\leq 150$  kHz and summed up.

For the experimental geometry of our choice,  $\mathbf{H} \perp [0\bar{1}1]$ ,  $\angle(\mathbf{H}, \mathbf{a}^*) = 45^\circ$ , the  $^{13}\text{C}$  NMR spectrum measured in the metallic state of the title compound

is a single resonance line, as exemplified in Fig. 3c. In theory, for the given field orientation one expects a

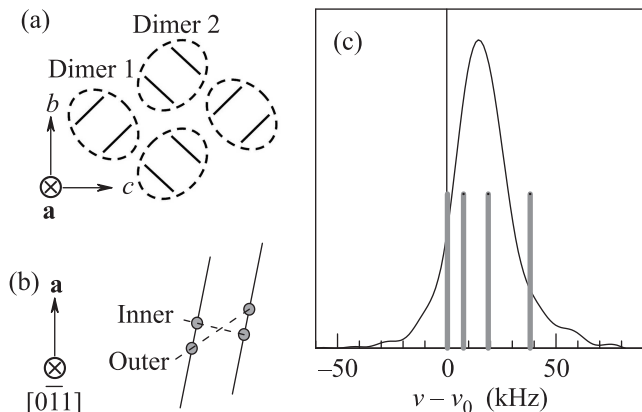


Fig. 3. (a) – Schematic top view of the conducting BETS layer.  $(\text{BETS})_2$  dimers are represented by the pairs of lines. (b) – Schematic side view of a BETS dimer with site definition of the central carbons; (c) –  $^{13}\text{C}$  NMR spectrum measured at  $T = 50$  K in the external field  $\mu_0 H = 7$  T aligned perpendicular to  $[0\bar{1}1]$  at  $45^\circ$  to  $\mathbf{a}^*$ . The spectrum is shown with respect to  $\nu_0 = 74.946$  MHz. Grey vertical lines indicate positions of the resonance peaks calculated with the shift tensor of  $\kappa\text{-(ET)}_2\text{Cu[N(CN)}_2\text{]Br}$

$\kappa\text{-(BETS)}_2\text{Mn[N(CN)}_2\text{]}_3$  crystal to produce four  $^{13}\text{C}$  NMR peaks [15]. They arise from the two magnetically different orientations of the BETS dimers in the unit cell, as shown in Fig. 3a, and nonequivalent (‘inner’ and ‘outer’) central carbon sites within the dimers, Fig. 3b. The BETS molecules within the dimer are inversion-symmetric to each other, thus magnetically equivalent. The dipolar interaction between the spins of the central  $^{13}\text{C}$ , which in general provides another factor of two to the number of peaks, is nearly zero for this field orientation.

In order to calculate the positions of the four peaks one needs to know the values of the  $^{13}\text{C}$  shift tensors for the ‘inner’ and ‘outer’ carbon sites in  $\kappa\text{-(BETS)}_2\text{Mn[N(CN)}_2\text{]}_3$ . The total shift tensor is composed of the chemical (orbital), Knight (spin), and “dipolar” shift tensors. The dipolar contribution resulting from the dipolar fields induced by  $\text{Mn}^{2+}$  moments can be calculated following Ref. [10], using the measured dc magnetization values [2]. The former two contributions, which characterize, respectively, the intrinsic fields within the BETS molecule itself and the fields induced by the spins of conduction electrons, are currently unknown. Assuming that the tensors are similar to those in the ET-based compounds (ET is isostructural to BETS but with sulphur on Se sites), we use the values obtained for  $\kappa\text{-(ET)}_2\text{Cu[N(CN)}_2\text{]Br}$  [15] to cal-

culate the  $^{13}\text{C}$  NMR peak positions. The resulting peak positions (including the dipolar shift) are indicated in Fig. 3c by grey vertical lines. One can see that the resonance line observed in the experiment covers fairly well the range of the calculated peak positions, indicating that the  $^{13}\text{C}$  shift tensor in  $\kappa\text{-(BETS)}_2\text{Mn[N(CN)}_2\text{]}_3$  is not much different from that in  $\kappa\text{-(ET)}_2\text{Cu[N(CN)}_2\text{]Br}$ .

Evidently, the peaks from individual carbon sites in the metallic state of  $\kappa\text{-(BETS)}_2\text{Mn[N(CN)}_2\text{]}_3$  are vastly broadened and merged into a single line. An excessive broadening of  $^{13}\text{C}$  NMR peaks has been noticed in  $\kappa\text{-(ET)}_2\text{Cu[N(CN)}_2\text{]Br}$  below  $T = 150$  K, and a number of reasons has been recruited to explain it, including spacial variation of the  $\pi$ -electron spin density due to precursors to Anderson localization or a spin-density wave [15]. Minor sample imperfection, which cannot be ruled out, may also contribute to the linewidth because each of the three contributions to the total shift mentioned above are highly anisotropic, while the dipolar shift is also sensitive to atomic displacements [10]. More detailed analysis of possible broadening mechanisms in the metallic state is beyond the scope of this communication.

The shape of the  $^{13}\text{C}$  NMR spectrum changes rapidly as the system enters the insulating state. The left panel in Fig. 4 shows  $^{13}\text{C}$  NMR spectra measured in  $\kappa\text{-(BETS)}_2\text{Mn[N(CN)}_2\text{]}_3$  at temperatures from 5 to 50 K at ambient pressure. The single peak characteristic of the spectrum in the metallic state above  $T = 23\text{ K} \approx T_{\text{MI}}$ , develops below this temperature into a broad symmetric pattern counting 5 peaks at least. At  $T = 5$  K the spectrum spans a range of nearly  $\pm 1$  MHz which is huge compared to the spectrum in the metallic state. This cannot result from the dipolar fields created by  $\text{Mn}^{2+}$ : calculations show that fully polarized  $\text{Mn}^{2+}$  can provide a dipolar shift ranging from  $-12.5$  to  $-19$  kHz (depending on the carbon site) in a 7 T field. Therefore, the spectrum below  $T_{\text{MI}}$  evidences an enhancement of the hyperfine field experienced by the  $^{13}\text{C}$  nuclear spin due to localization of the  $\pi$ -electron spins on the dimers of the BETS molecules. Moreover, several pronounced peaks are visible in the low-temperature spectrum, which infers a commensurate order of the localized spins. Finally, the symmetric shape of the spectrum indicates the staggered order, because antiparallel components of the staggered electron spins ( $\hat{\mathbf{S}}_i = -\hat{\mathbf{S}}_j$ ) produce opposite local fields at carbon sites  $i$  and  $j$ :  $h_i = \hat{\mathbf{I}}_i \cdot \mathbf{A} \cdot \hat{\mathbf{S}}_i = -(\hat{\mathbf{I}}_j \cdot \mathbf{A} \cdot \hat{\mathbf{S}}_j) = -h_j$ , where  $\hat{\mathbf{I}}$  and  $\hat{\mathbf{S}}$  are the nuclear and electron spin operators, respectively, and  $\mathbf{A}$  is the hyperfine tensor. In turn, this signifies the AF interaction between the localized spins. The staggered component of the spin magnetization should lie somewhere in the plane perpendicular to the mag-

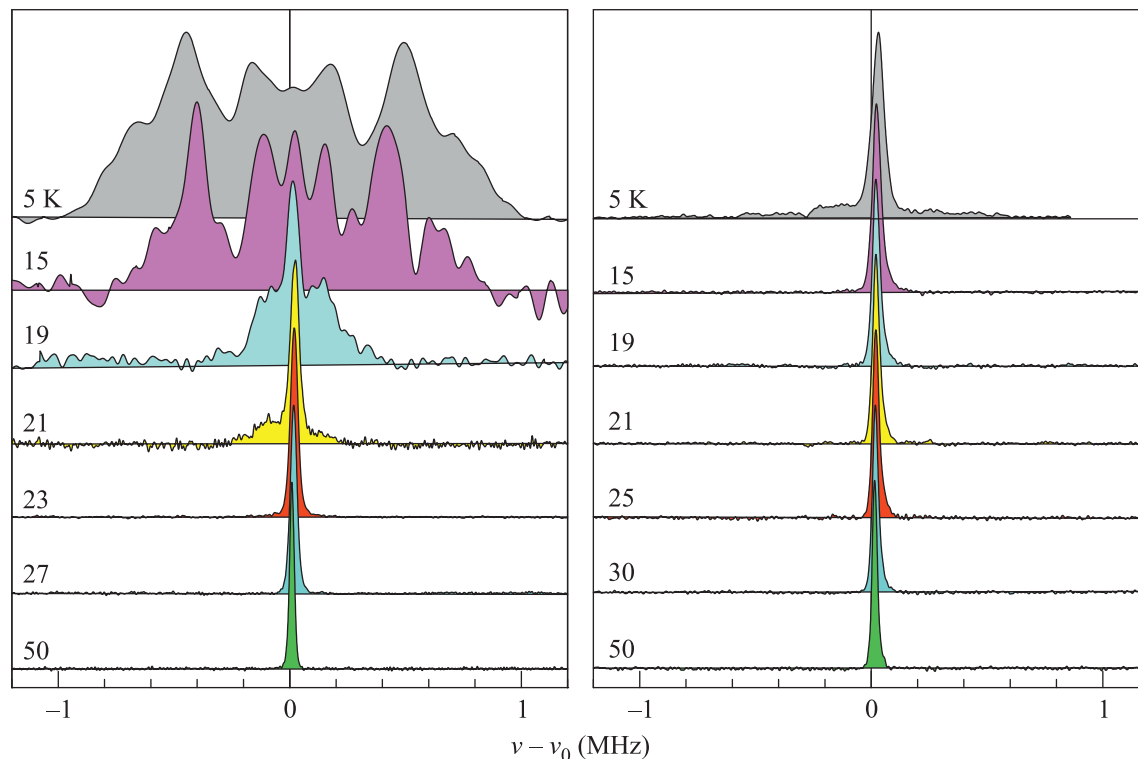


Fig. 4.  $^{13}\text{C}$  NMR spectra measured in  $\kappa\text{-(BETS)}_2\text{Mn}[\text{N}(\text{CN})_2]_3$  at several temperatures at ambient pressure,  $P = 0$  (left), and in GKZh-136,  $P \sim 0.5$  kbar (right)

netic field, since the anisotropic exchange term is usually much smaller than the external field  $\mu_0 H = 7$  T.

These signs of the commensurate staggered spin order are only present in the insulating state of  $\kappa\text{-(BETS)}_2\text{Mn}[\text{N}(\text{CN})_2]_3$ . The right panel in Fig. 4 shows the spectra for the sample submerged in GKZh. According to the resistance measurements (Fig. 2), the MI transition in this case is substantially suppressed due to the pressure ( $P \sim 0.5$  kbar) imposed to the sample by thermal contraction of GKZh. The narrow-peak spectrum characterizing the metallic state, obviously survives way below 23 K. Only at  $T = 5$  K the broad features show up, reminiscent of the ambient-pressure spectrum at  $T = 21$  K.

Therefore, the discovered staggered order of the localized spins is obviously related to the insulating state of  $\kappa\text{-(BETS)}_2\text{Mn}[\text{N}(\text{CN})_2]_3$  (cf. Figs. 2 and 4). First, it arises at the MI transition temperature. Secondly, it is suppressed by the external pressure in the same way as the MI transition. It is evident therefore that the staggered order occurs within the spin system of  $\pi$  electrons which localize on the dimers of the BETS molecules below  $T_{\text{MI}}$ . This finding provides a strong support in favor of an AF Mott-insulating state as a ground state of  $\kappa\text{-(BETS)}_2\text{Mn}[\text{N}(\text{CN})_2]_3$ .

The frequency range of the  $^{13}\text{C}$  spectrum in  $\kappa\text{-(BETS)}_2\text{Mn}[\text{N}(\text{CN})_2]_3$  at  $T = 5$  K measured at ambient pressure (left panel in Fig. 4) is of the same order of magnitude ( $\pm 1$  MHz) as in the AF Mott state of  $\kappa\text{-(ET)}_2\text{Cu}[\text{N}(\text{CN})_2]\text{Cl}$  [16] and  $\beta'\text{-(ET)}_2\text{ICl}_2$  [17]. A magnitude of the electron spin magnetization of  $0.5 \mu_B$  and  $1 \mu_B$  per dimer, respectively, has been reported for these two compounds. It should be within the same range here, since the hyperfine tensor in  $\kappa\text{-(BETS)}_2\text{Mn}[\text{N}(\text{CN})_2]_3$  is expected to be similar, as the measurements in the metallic phase suggest. It should be noted however that the staggered spin structure discovered in the present compound does not necessarily signify the conventional Néel AF state but can be a field-induced effect, as it occurs in  $\kappa\text{-(ET)}_2\text{Cu}[\text{N}(\text{CN})_2]\text{Cl}$  above  $T_N$  [18].

The staggered spin structure of the localized  $\pi$  electrons can be responsible for the magnetic effect observed in the  $3d$   $\text{Mn}^{2+}$  electron spin system. The behavior of the  $\text{Mn}^{2+}$  system below  $T_{\text{MI}}$  examined by the static magnetization and  $^1\text{H}$  NMR measurements [10, 2] infers some disordered tilt of the static component of  $\text{Mn}^{2+}$  moments from the external field direction. This can be interpreted as a trend of the  $\text{Mn}^{2+}$  system towards AF order, frustrated geometrically by the tri-

angular arrangement of Mn in the anion layer. However, the susceptibility of  $\kappa$ -(BETS)<sub>2</sub>Mn[N(CN)<sub>2</sub>]<sub>3</sub> determined by the Mn<sup>2+</sup> spin system, depends on temperature as  $(T+\theta)^{-1}$  with  $\theta \approx 5.5$  K [2], which implies a paramagnetic state of the Mn<sup>2+</sup> subsystem down to  $T \sim \theta$ . In fact, it deviates from the paramagnetic behavior at much higher temperature  $T_{\text{MI}} \sim 23$  K. One can assume therefore that it is the ordered  $\pi$ -spin system that affects the paramagnetic state of Mn<sup>2+</sup> spins via the  $\pi$ - $d$  interactions. The disorder in the frustrated Mn<sup>2+</sup> system, in turn, introduces some disorder in the  $\pi$ -spin structure. Comparing <sup>13</sup>C NMR spectra taken at 5 and 15 K at ambient pressure (left panel in Fig. 4), one can notice that the positions of the resonance peaks are nearly the same, indicating a nearly constant magnitude of the electron spin magnetization, while the peak widths are much bigger at  $T = 5$  K. It is possible that the disordered Mn<sup>2+</sup> spins whose magnetization grows in this temperature region by a factor of two [2], induce some disorder in the orientations of the  $\pi$ -spins. In other words, the trend of the Mn<sup>2+</sup> spins to follow the AF arrangement of the  $\pi$ -spins is frustrated by the triangular network of Mn, which in turn leads to some disorder of the  $\pi$ -spins as well.

Indeed, determining the spin structure of the localized  $\pi$ -electrons would be of great importance. To do this one needs to derive from the NMR data the hyperfine tensors for the central carbons in  $\kappa$ -(BETS)<sub>2</sub>Mn[N(CN)<sub>2</sub>]<sub>3</sub>. This requires the value of the  $\pi$ -spin susceptibility which, to our knowledge, has never been reported so far. An appropriate technique to measure this value would be ESR, provided that the resonance peaks from Mn<sup>2+</sup> and  $\pi$ -electron spins are resolved. Besides, ESR could give information about the low-field spin structure of the localized  $\pi$ -electrons, such as the orientation of the easy-axis (if exists).

In conclusion, we performed <sup>13</sup>C NMR measurements on the central carbons of the BETS molecules in  $\kappa$ -(BETS)<sub>2</sub>Mn[N(CN)<sub>2</sub>]<sub>3</sub> with and without the external pressure to retrieve the spin properties of the conduction  $\pi$ -electrons. We found that the transition of the system into the insulating state is accompanied by ordering of the  $\pi$ -spins into a long-range staggered structure. This supports the assumption that the MI transition is due to Mott instability resulting from strong correlations within the half-filled band conduction electron system. The staggered  $\pi$ -spin structure is suggested to be respon-

sible for the changes in the Mn<sup>2+</sup> spin system observed in the static magnetization and <sup>1</sup>H NMR experiments.

The authors thank R. Kato for providing <sup>13</sup>C-labeled BETS. We gratefully acknowledge fruitful suggestions from S.E. Brown, the assistance in questions of crystallography from S.V. Simonov, and technical support from N.A. Belov. This work was supported by the RFBR grants # 10-02-01202 and 11-02-91338-DFG (DFG grant # Bi 340/3-1) and the Russian State Contract # 14.740.11.0911.

1. N. D. Kushch, E. B. Yagubskii, M. V. Kartsovnik et al., *J. Am. Chem. Soc.* **130**, 3278 (2008).
2. O. M. Vyaselev, M. V. Kartsovnik, W. Biberacher et al., *Phys. Rev. B* **83**, 094425 (2011).
3. V. N. Zverev, M. V. Kartsovnik, W. Biberacher et al., *Phys. Rev. B* **82**, 155123 (2010).
4. H. Kobayashi, H. Tomita, T. Naito et al., *J. Am. Chem. Soc.* **118**, 368 (1996).
5. H. Kobayashi, H. B. Cui, and A. Kobayashi, *Chem. Rev.* **104**, 5265 (2004).
6. S. Uji and J. S. Brooks, *J. Phys. Soc. Jpn.* **75**, 051014 (2006).
7. L. Brossard, R. Clerac, C. Coulon et al., *Eur. Phys. J. B* **1**, 439 (1998).
8. H. Akiba, S. Nakano, Y. Nishio et al., *J. Phys. Soc. Japan* **78**, 033601 (2009).
9. J. C. Waerenborgh, S. Rabaça, M. Almeida et al., *Phys. Rev. B* **81**, 060413(R) (2010).
10. O. M. Vyaselev, N. D. Kushch, and E. B. Yagubskii, *Zh. Eksp. Teor. Fiz.* **140**, 961 (2011) [*JETP* **113**, 835 (2011)].
11. F. Kagawa, K. Miyagawa, and K. Kanoda, *Nature Physics* **5**, 880 (2009).
12. T. Klutz, I. Hennig, U. Haeberlen et al., *App. Mag. Res.* **2**, 441 (1991).
13. N. D. Kushch, L. I. Buravov, A. N. Chekhlov et al., *J. Sol. State Chem.* **184**, 3074 (2011).
14. L. I. Buravov, A. V. Kazakova, N. D. Kushch et al., *Instr. Exp. Techn.* **51**, 156 (2008).
15. S. M. De Soto, C. P. Slichter, A. M. Kini et al., *Phys. Rev. B* **52**, 10364 (1995).
16. D. F. Smith, S. M. De Soto, C. P. Slichter et al., *Phys. Rev. B* **68**, 024512 (2003).
17. Y. Eto and A. Kawamoto, *Phys. Rev. B* **81**, 020512 (2010).
18. F. Kagawa, Y. Kurosaki, K. Miyagawa et al., *Phys. Rev. B* **78**, 184402 (2008).